Communications in Physics, Vol. 34, No. 3 (2024), pp. 277-288
DOI: https://doi.org/10.15625/0868-3166/20630

Transformation of ferromagnetic properties in Fe_3O_4 to α-Fe_2O_3 by the polyol process and heat treatment

Nguyen Thi Nhat Hang[1], **Le Hong Phuc**[2], **Ho Van Cuu**[3], **Nguyen Huu Tri**[3] **and Nguyen Viet Long**[3,†]

[1]*Institute of Applied Technology, Thu Dau Mot University, 6 Tran Van On Street, Phu Hoa Ward, Thu Dau Mot City 820000, Vietnam*

[2]*National Institute of Applied Mechanics and Informatics, Vietnam Academy of Science and Technology, 291 Dien Bien Phu, Ho Chi Minh City, 700000, Vietnam*

[3]*Department of Electronics and Telecommunications, Saigon University, 273 An Duong Vuong, District 5, Ho Chi Minh City 700000, Vietnam*

E-mail: †nguyenvietlong@sgu.edu.vn

Received 23 April 2024

Accepted for publication 17 July 2024

Published 24 July 2024

Abstract. *This study investigates the transformation of ferromagnetic properties of Fe_3O_4 to α-Fe_2O_3 through the polyol process and subsequent heat treatment. Structural and magnetic changes were analyzed via X-ray diffraction (XRD), scanning electron microscopy (SEM), and vibrating sample magnetometer (VSM), revealing significant phase transitions and magnetic property variations.*

Keywords: polyol process; polyol technology; α-Fe_2O_3; Fe_3O_4; ferromagnetism.

Classification numbers: 75.50.Gg.

1. Introduction

At present, Fe-, Co-, Ni-, Fe_2O_3-, and Fe_3O_4-based magnetic materials have various applications for life, energy, environment, medicine and biology, especially for modern devices and components in electronics and telecommunications [1, 2]. Their controlled synthesis and magnetic properties are very attractive to researchers [1, 2]. In recent years, micro/nanostructured magnetic products of Fe-based oxide materials have been widely studied. Therefore, there are the various classes of Co-, Fe-, Ni-based magnetic micro/nanosized metal, alloy, and oxide materials,

exhibiting special magnetic properties that are paramagnetic, diamagnetic, ferromagnetic, antiferromagnetic, ferrimagnetic, soft and hard magnetic, respectively [1–4]. Micro/nanosized Fe_3O_4 oxides have been discussed in detail for biomedical applications [3,4]. Therefore, the kinds of micro/nanosized Fe_3O_4 and α-Fe_2O_3 oxides were developed [5,6]. The structural kinds of γ-Fe_2O_3 and α-Fe_2O_3 oxides have the stable magnetic properties [7]. So, micro/nanosized Fe_3O_4 and α-Fe_2O_3 can be used for potential applications in biomedicine, energy and environment [8, 9]. In nature, the mineral evidence of Fe_3O_4 (magnetite) and α-Fe_2O_3 (hematite) oxides were found in comparison with their synthesis in Labs [10–18]. There are many various methods and processes for synthesis, such as combustion methods and other chemical, physical methods [19, 20]. The polyol process shows great advantages for the synthesis of magnetic nanoparticles and nanostructures from Fe-, Ni-, and Co-based precursors, solvents, and solutions [21]. A modified polyol process has also been used with strong reducing agents, i.e. $NaBH_4$ in EG (or PolyEG) [22, 23]. Thus, micro/nanosized ferrites and hexaferrites can be realized by the polyol process or the emerging polyol technology [22, 24]. The core-shell α-Fe_2O_3/Fe_3O_4 oxide was used for photocatalysis for environments [25]. Most of micro/nanosized Fe_3O_4 and Fe_2O_3/Fe_3O_4 have been developed for batteries, capacitors, and fuel cells [25–30]. They are micro/nanosized magnetic materials in the various forms of iron oxides, ferrites, and hexaferrites used in practical devices, typically such as recorders, televisions, refrigerators, electric fans, motorbikes, cars, telephones, toys, magnetic records, and magnetic memory [1–3]. In particular, Fe_3O_4 and α-Fe_2O_3 are also potentially used in medical and biomedical applications in the treatment of toxic cancers and tumors [3]. Micro/nanosized iron oxides can certainly be synthesized by the polyol processes, heat treatment, annealing and sintering. To develop Fe oxide materials in the designed micro/nanosized ranges, we need to focus on two of the most common types of micro/nanosized Fe_3O_4 and α-Fe_2O_3 oxides. Here, they are the most important source materials used to make the most of advanced iron oxide materials, such as ferrites and hexaferrites. There are many preparation methods for obtaining the kinds of FeO (wüstite), Fe_3O_4, Fe_2O_3, or Fe_xO_y magnetic materials. Micro/nanosized magnetic oxide materials are the starting material to form magnetic alloy and oxide materials at high-temperature processes that are applied to the manufacture of magnetic recording materials and magnetic spintronics. It is known that FeO, Fe_2O_3, and Fe_3O_4 show the general formula Fe_xO_y ($x+y=2$, 5 and 7 for original magnetic structures) needed to study in understanding their structure and magnetic properties by various synthetic methods, such as chemistry, physics, and other physical/chemical methods. In the practical aspects of micro/nanosized magnetic materials, the kinds of magnetic oxide particles in the various forms of Fe_3O_4 and α-Fe_2O_3 have been effectively synthesized by $FeCl_3$ (or/and $FeCl_2$), PVP, EG, and other controlling agents. Most importantly, strong reducing agent is used to be $NaBH_4$. The heat treatment, annealing and sintering processes are used for final products of the various kinds of Fe-, Co-, and Ni-based micro/nanosized magnetic oxides [22, 23, 31, 32].

In this study, we have mainly focused on in-depth research on the synthesis of Fe_3O_4, and the significant structural change from the crystal structure of Fe_3O_4 into the crystal structure of α-Fe_2O_3 through annealing and sintering. We have also provided the fabrication of magnetic oxide nanomaterials, structures, properties, shapes and sizes of Fe_3O_4 and α-Fe_2O_3 micro/nano oxide particles. In this context, micro/nanosized Fe_3O_4 oxides of ferromagnetic properties were synthesized by polyol process and heated to change ferromagnetism into parasitic ferromagnetism of micro/nanosized α-Fe_2O_3. The strong phase transition from ferromagnetism of Fe_3O_4 into

ferromagnetism of α-Fe_2O_3. Finally, the magnetization process and hysteresis loops were studied in detail based on the experiments performed.

2. Experiment

In our typical polyol processes, the chemical used for synthesis was $FeCl_3$ (0.0625M) (China, AR, CAS:10025-77-1; characteristic: yellow-brown crystals. Readily deliquescent in air), NaOH (0.0625M) (China, AR, CAS: 1370-73-2; characteristic: white uniform granular or flaky solid), EG (China, AR, CAS: 107-21-1), PVP (0.375M) (China, AR), $NaBH_4$ (China, AR, CAS: 16940-66-2; appearance: white powder) purchased from industrial chemicals, following laboratory and industrial manufacturing approach. In the experiments, $FeCl_3$ (0.0625M) can be separately used for synthesis (or $FeCl_3$ (0.0625M) can be replaced by $FeCl_2$ (0.0625M)) (or both $FeCl_2$ and $FeCl_3$ were simultaneously used) according to the lab skills and experiences of the experimenter and the designed polyol processes [22, 23, 32, 33]. All the experiments synthesizing the kind of micro/nanosized Fe_3O_4 oxides of ferromagnetism, and the kind of micro/nanosized α-Fe_2O_3 oxides of ferromagnetism, were synthesized under the experimental conditions in the laboratory. The details of the chemical preparation, synthesis, and sample cleaning procedures have been described in previous studies [32, 33]. Next, the above powders were used for experimental measurements, the oxide powder samples were dried at a low temperature of 100˚C, isothermally sintered, crystallized at higher temperatures up to 950˚C, and cooled to room temperature.

The dried powder samples were heated and sintered in the temperature range of 100-950˚C using a high-temperature furnace with a temperature range according to the annealing temperature points from room temperature to 950˚C for full densification in phase identification of α-Fe_2O_3 oxides. To investigate the types of as-prepared micro/nanosized Fe_3O_4 and α-Fe_2O_3 oxides, the most typical samples selected were used, which were prepared by heat processes and isothermally heated from low to high temperatures in air. The annealing temperature points used were approximately 100, 200, 300, 400, 500, 600, 700, 800, 900, and 950˚C for making the samples in a period of approximately 2h. The samples were labeled to be (1), (2), (3), (4), (5), (6), (7), (8), (9) and (10), respectively.

Additionally, X-ray diffraction (XRD), scanning electron microscopy (SEM), and vibrating sample magnetometer (VSM) measurements at room temperature were used to prove the crystal structures and related magnetic properties, respectively. Typically, the features of ferromagnetism and hysteresis loops of M-H of micro/nanosized Fe_3O_4 and α-Fe_2O_3 powders were measured using a VSM, EZ9 Vibrating Sample Magnetometer (VSM, MicroSense, LLC Corporation, USA), and demagnetization field (Hc) in the range of -1500 to +1500 Oe. The crystal structures of the as-prepared samples (micro/nanosized Fe_3O_4 and α-Fe_2O_3 powders) were investigated using XRD (Empyrean PANalytical diffractometer, USA).

In the particle size analysis of the image data, the as-prepared Fe_3O_4 and α-Fe_2O_3 powders were primarily investigated using ultrahigh-resolution scanning electron microscopy (FESEM, S-4800, Japan) to study their micro/nanosized textures and surface analysis. In addition, SEM (Tescan Mira, Czech Republic) was used with FEG Schottky electron emission source combined with SEM imaging and live elemental composition analysis. The resolution for imaging and EDS analysis was maintained to investigate the as-prepared micro/nanosized Fe_3O_4 and α-Fe_2O_3 oxide powders.

3. Results and discussion

3.1. XRD: Crystallization

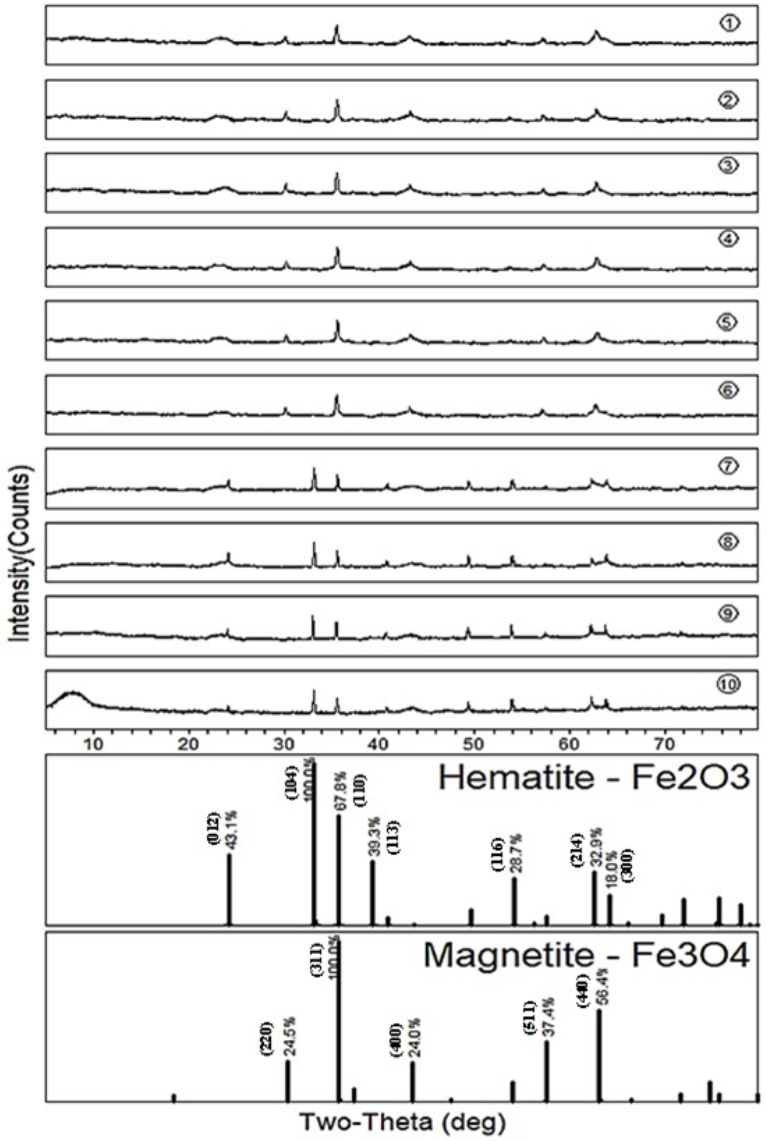

Fig. 1. The typical XRD measurements of Fe_3O_4 and α-Fe_2O_3 oxides, and the typical samples of micro/nanosized Fe oxides heated at 100, 200, 300, 400, 500, 600, 700, 800, 900, and 950˚C from top to bottom (from Sample 1 to Sample 10) by the polyol process, heat treatment, annealing and sintering for the periods of 2h.

Figure 1 shows the as-prepared iron oxides including Fe_3O_4 and α-Fe_2O_3 according to the two standard patterns (PDF#75-1609: Magnetite, Syn, Fe_3O_4, Cubic, Fd-3m(227); PDF#86-0550:

Hematite, α-Fe_2O_3, Rhombohedral, R-3c(167)), respectively. In the certain range of annealing temperatures from 100 to 600˚C, Fe_3O_4-type micro/nanosized iron oxides were identified in the main forms of magnetite-Fe_3O_4-type structures. The strong lines of a set of (hkl) Miller index of magnetite-Fe_3O_4-type crystal oxides include (011), (112), (103), (004), (132), (321), (440), and other (hkl) planes corresponding to the values of 2T (˚) of 18.453, 30.269, 35.664, 43.317, 53.696, 57.258, 62.865, and other 2T values, respectively. The results are in agreement with the standard patterns of PDF#75-1609. The strongest line in the XRD spectrum is (103) and 100% of intensity, and the percent of intensity of the (hkl) lines were shown. Interestingly, the significant crystal changes of Fe_3O_4 into α-Fe_2O_3 in high crystallization were discovered in our evidence of the as-prepared samples of micro/nanosized Fe oxides between 600 and 700˚C. The strong lines of a set of (hkl) Miller index of hematite-Fe_2O_3-type crystal oxides include (012), (104), (110), (113), (024), (116), (122), (214), (300), (1010), and other (hkl) planes corresponding to 2T values 24.160, 33.150, 35.593, 40.824, 49.397, 54.007, 57.543, 62.339, 63.887, 71.859, and other 2θ values, respectively. The results are in agreement with the standard patterns of PDF#86-0550. The strongest line in the XRD spectrum is (104) considered to be 100% of intensity. The minor intensities of other (hkl) planes in the diagrams can be ignored. In the range of annealing temperatures from 700 to 950˚C (Fig. 1), the crystal formation processes of α-Fe_2O_3-type micro/nanosized iron oxides were fully identified in the main forms of hematite-α-Fe_2O_3-type crystal structures.

It is clearly known that FeO (Fe^{2+} valence), has a cubic crystal structure, is non-magnetic or weak magnetic, and difficult to detect. However, it is suggested that Fe_2O_3 oxides show a state of Fe^{3+} valence that can form stable α-Fe_2O_3 and γ-Fe_2O_3 oxides. They often have an orthorhombic structure. In this study, when heating the above two types, α-Fe_2O_3 was obtained which was very stable at high temperatures. As a result, heating and annealing temperatures are less than 1000˚C. There is a more general formula for the Fe_xO_y system as mFeO.$n$$Fe_2O_3$, leading to a diversity of Fe_3O_4, α-Fe_2O_3 and γ-Fe_2O_3 oxides in the research and synthesis of nano/microsized ferromagnetic oxides.

3.2. VSM: Ferromagnetism

Figure 2 shows the typical VSM measurements of micro/nanosized Fe oxides of the kinds of Fe_3O_4 and α-Fe_2O_3 oxides, and the typical samples of micro/nanosized Fe oxides heated at 100, 200, 300, 400, 500, 600, 700, 800, 900, and 950˚C by the polyol process and heat treatment for 2h. It is confirmed that the fabricated micro/nanosized Fe oxides of Fe_3O_4 and α-Fe_2O_3 exhibit remanent magnetic properties during the measured hysteresis cycles. Therefore, the fabricated samples have remanence, i.e. Mr., i.e. H = 0, the as-prepared Fe oxide samples that kept their magnetism. Fig. 2 also shows that the fabricated samples of micro/nanosized Fe_3O_4 oxides have ferromagnetic properties in the sample-fabrication temperature range from 100 to 600˚C.

In this temperature range, hysteresis loops can be explained by the two stages. The first stage is when magnetic walls are moved under the external magnetic field H. The next stage is that spin rotation is strongly dependent on H. In particular, the magnetic properties of micro/nanosized α-Fe_2O_3 oxides are popular in the temperature range from 700 to 950˚C, which were relatively complex and abnormal. The phenomenon of ferromagnetism of Fe_3O_4 changing into ferromagnetism of α-Fe_2O_3 due to the structural change from Fe_3O_4 to Fe_2O_3 is a typical property of ferromagnetic micro/nanosized materials explained by Weiss's natural magnetization domain theory, which are soft ferromagnetic materials (Figs. 1 and 2).

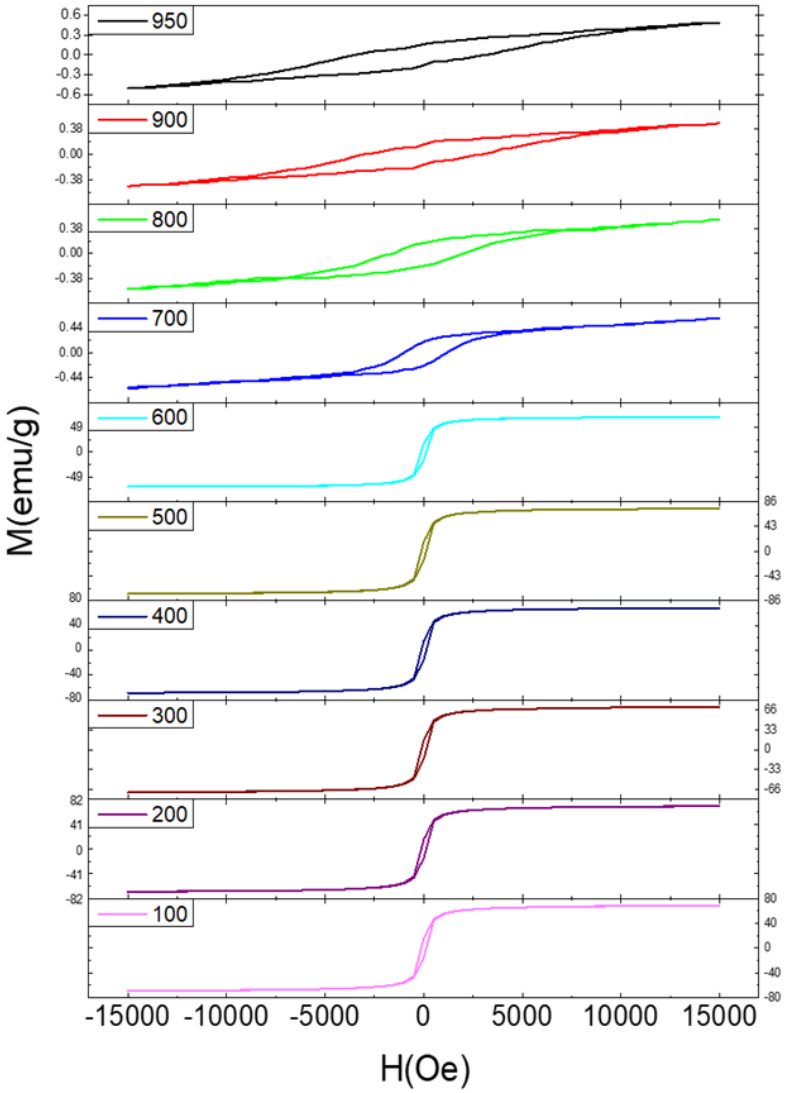

Fig. 2. The typical VSM measurements of Fe_3O_4 and α-Fe_2O_3 oxides, and the samples of micro/nanosized Fe oxides heated at 100, 200, 300, 400, 500, 600, 700, 800, 900, and 950˚C by the polyol process, heat treatment, annealing and sintering for 2h.

Basically, the most typical ferromagnetic parameters of the hysteresis loops of micro/nanosized Fe_3O_4 oxides, and micro/nanosized α-Fe_2O_3 oxides include Ms (saturation magnetization), Mr (remanent magnetization of M at H = 0), Hc (applied field at which M/H changes sign), and S (squareness S is determined by taking the ratio Mr/Ms), respectively. The typical values of S of soft, soft/hard, semi-hard, and hard magnetic micro/nanosized materials tend to go to be 1.0 for most of the best hard magnetic materials expected [33]. The ferromagnetic parameters of micro/nanosized Fe_3O_4 and α-Fe_2O_3 oxides are estimated in Tables 1 and 2. It is also noted that the

magnetization process was mostly irreversible, leading to the values of Mr (remanence) that were identified in the experimental measurements by VSM in this study.

Table 1. The averaged values of magnetic parameters of micro/nanosized Fe_3O_4.

Samples	S100	S200	S300	S400	S500
Temp. (^{o}C)	100	200	300	400	500
Hc (Oe)	127.44	125.64	125.05	123.99	124.12
Mr (emu/g)	15.48	15.39	15.44	14.88	15.91
Ms (emu/g)	68.65	70.61	70.39	68.40	73.61
S (Mr/Ms)	0.23	0.22	0.22	0.22	0.22

Table 2. The averaged values of magnetic parameters of micro/nanosized Fe_3O_4 and α-Fe_2O_3 oxides.

Samples	S600	S700	S800	S900	S950
Temp. (^{o}C)	600	700	800	900	950
Hc (Oe)	133.89	1083.37	1750.03	3000.07	3250.06
Mr (emu/g)	16.38	0.21	0.12	0.15	0.16
Ms (emu/g)	68.09	0.61	0.52	0.48	0.49
S (Mr/Ms)	0.24	0.35	0.22	0.32	0.32

It is experimentally evidenced that micro/nanosized Fe_3O_4 oxides have high values of Ms from 68.09 to 73.61 emu/g in Tables 1 and 2 (S100-S600 with respect to the samples heated at 100, 200, 300, 400, 500, and 600˚C), and micro/nanosized α-Fe_2O_3 oxides have the low values of Ms from 0.48 to 0.61 emu/g (S700-S950) in respect with the samples heated at 700, 800, 900, and 950˚C).

The important variation of structure and magnetism from Fe_3O_4 into α-Fe_2O_3 was observed in a change of small temperature range from 600˚C to 700˚C.

The magnetic parameters of Fe_3O_4 oxides (heated at 100˚C) and α-Fe_2O_3 oxides (heated at 950˚C) were listed in Tables 1 and 2. The values of Hc of α-Fe_2O_3 oxides for the samples isothermally heated at high temperatures for 2h are 25.5 times higher than those of Hc of Fe_3O_4 oxides due to the difference in their magnetic structure.

However, the average values of Mr, and Ms of Fe_3O_4 oxides were 96.75, and 140 times more than those of Mr, and Ms of α-Fe_2O_3 oxides, respectively. The stability and durability of crystal structure and magnetic property of micro/nanosized Fe_3O_4 oxides need to be used in a temperature range from 100 to 600˚C for 2h.

Therefore, those of micro/nanosized α-Fe_2O_3 oxides need to be used in a temperature range from 700 to 950˚C for 2h in comparison with other different works [34, 35]. In this research, the values of Hc (about 1083-3250 Oe) is much higher than those of Hc (about 42.2-1459 Oe) [34] and

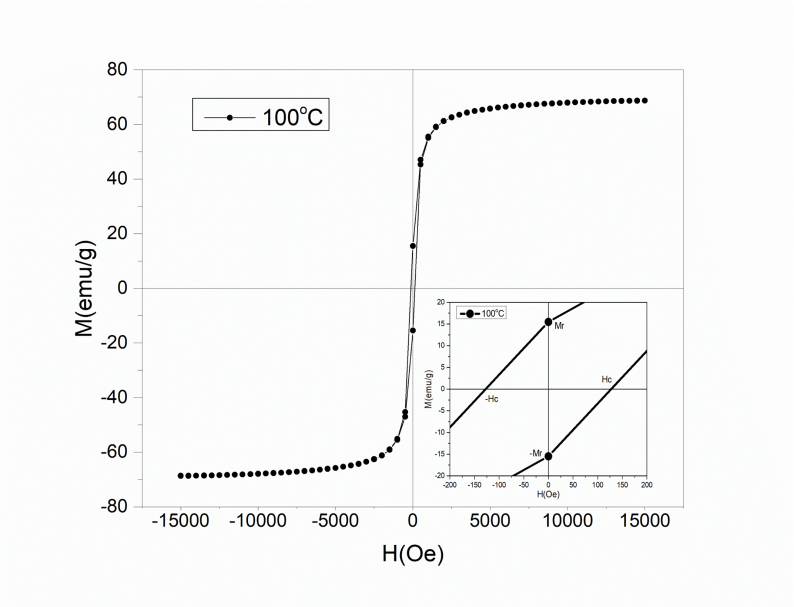

Fig. 3. The typical VSM measurements of Fe_3O_4 heated at 100°C by the polyol process and heat treatment for 2h.

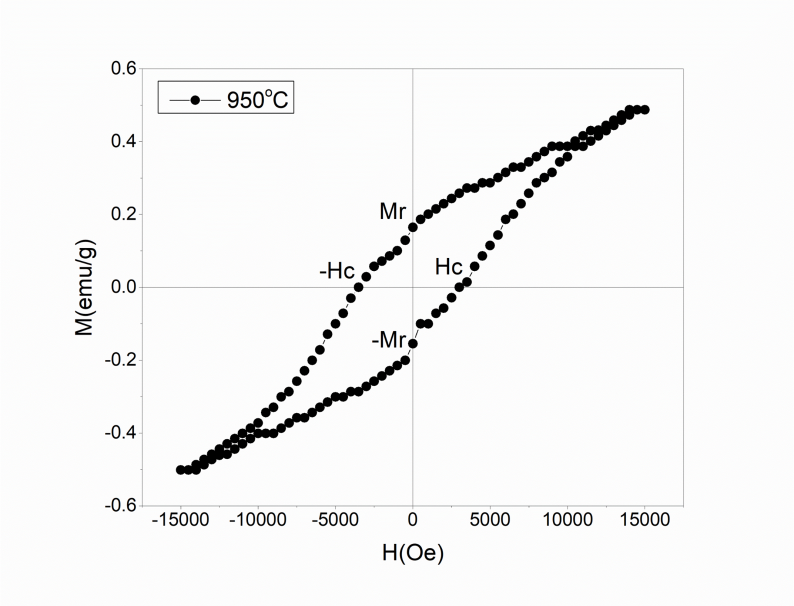

Fig. 4. The typical VSM measurements of α-Fe_2O_3 heated at 950°C by the polyol process and heat treatment for 2h.

magnetic measurements in cool conditions [35]. This proves that the as-prepared samples show magnetic property of high quality.

3.3. SEM: The issues of size, shape, and morphology

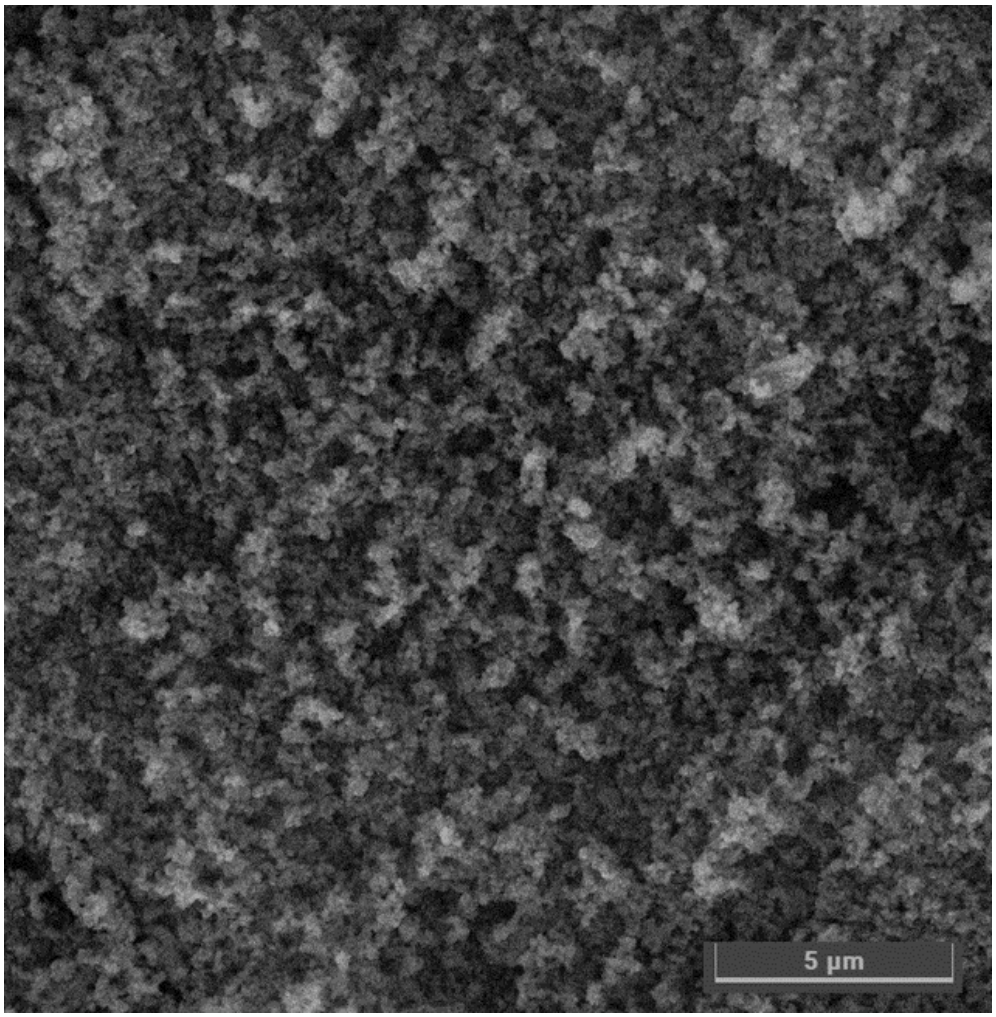

Fig. 5. Micro/nanosized Fe_3O_4-type particles heated at 100˚C for 2h by SEM (Scale bar: 5 μm).

Figure 5 shows the results of size, shape, and morphology of micro/nanosized Fe_3O_4-type Fe oxides (dried products) in the small fluctuation range of temperature around 100˚C. The samples were isothermally heated at 100˚C for 2h which led to obtain a particle powder product of Fe_3O_4 oxides in the range of micro/nanosized scales.

Similarly, Fig. 6 also shows the results of the size, shape, and morphology of micro/nanosized α-Fe_2O_3 oxides heated at 950˚C for 2h. In this case, the new, large, and special micro/nanotextures of small magnetic α-Fe_2O_3 oxide particles attached were formed around 950˚C due to their self-assembly by annealing and sintering at high temperatures [32, 33].

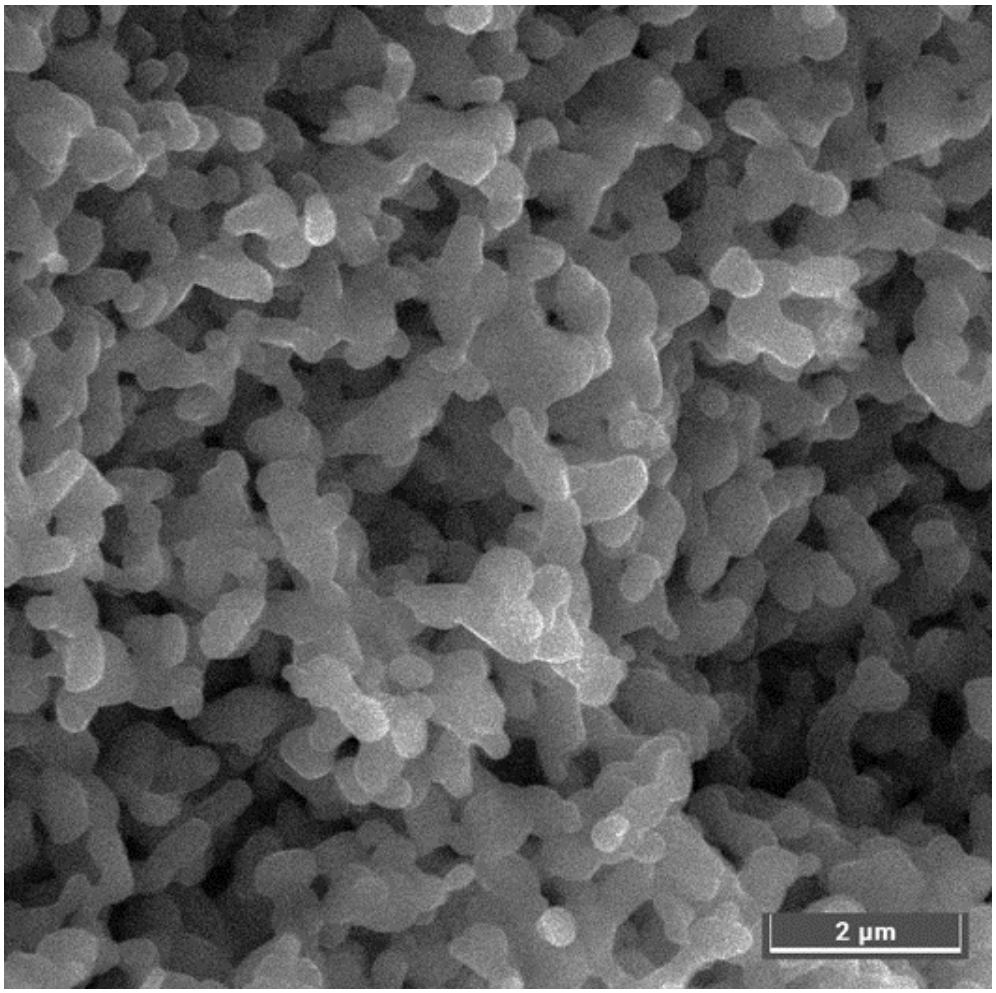

Fig. 6. Micro/nanosized Fe_3O_4 particles heated at 950˚C for 2h by SEM (Scale bar: 2 μm).

So far, the various kinds of micro/nanosized Fe_3O_4 and α-Fe_2O_3 oxides have been considered as potential promising candidates for our life, typically such as batteries, capacitors, energy, environment, and gas-sensing potential applications [23, 24].

4. Conclusion

In this study, magnetic phenomena according to magnetic crystal structures of micro/nanosized Fe_3O_4 and α-Fe_2O_3 oxides have been presented in experiments. The significant influences of temperature and manufacturing process on the magnetic properties of magnetic Fe oxides were confirmed, from the ferromagnetic properties of Fe_3O_4 to antiferromagnetic properties of α-Fe_2O_3. This is a good result for understanding the composition of other micro/nanosized magnetic materials dependent on heat treatment, annealing and sintering processes for preparing the next ferrites

and hexaferrites formed by the matrix of Fe_3O_4 ($FeO.Fe_2O_3$) and α-Fe_2O_3 because FeO can be replaced by MeO (Me: Fe, Ni, Co, Cu, Mg, etc) in the future.

Acknowledgment

This research was supported by Saigon University through Grant number CSB2022-54. N. V. Long is thankful to SGU University for funding.

Authors contributions

N.V.L. (author contribution: 90%) conducted all the experiments, collected the data and results, wrote the entire original manuscript, and evaluated and discussed the results and insights into the polyol processes for synthesis of micro/nanosized iron oxides, ferrites and hexaferrites oxides. L.H.P. (author contribution: 2.5%), N.H.T. (author contribution: 2.5%), N.T.N.H. (author contribution: 2.5%), and H.V.C. (author contribution: 2.5%) reviewed and discussed the research results. In many recent years, N.T.N.H. has funded TDMU University in her best efforts for a research program of nanoscience and nanotechnology. All the authors have read and agreed to the published version of the manuscript.

References

[1] K. Zhu, Y. Ju, J. Xu, Z. Yang, S. Gao and Y. Hou, *Magnetic nanomaterials: Chemical design, synthesis, and potential applications*, Acc. Chem. Res. **51** (2018) 404.

[2] A. Vedrtnam, K. Kalauni, S. Dubey and A. Kumar, *A comprehensive study on structure, properties, synthesis and characterization of ferrites*, AIMS Mater. Sci. **7** (2020) 800.

[3] M. D. Nguyen, H. V. Tran, S. Xu and T. R. Lee, *Fe_3O_4 nanoparticles: structures, synthesis, magnetic properties, surface functionalization, and emerging applications*, Appl. Sci. **11**(23) (2021) 11301.

[4] I. S. Lyubutin, C. R. Lin, Y. V. Korzhetskiy, T. V. Dmitrieva and R. K. Chiang, *Mössbauer spectroscopy and magnetic properties of hematite/magnetite nanocomposites*, J. Appl. Phys.**106** (2009) 034311.

[5] G. Tong, W. Wu, J. Guan, H. Qian, J. Yuan and W. Li, *Synthesis and characterization of nanosized urchin-like α-Fe_2O_3 and Fe_3O_4: microwave electromagnetic and absorbing properties*, J. Alloys Compd. **509**(11) (2011) 4320.

[6] J. S. Xu, Y. J. Zhu and F. Chen, *Solvothermal synthesis, characterization and magnetic properties of α-Fe_2O_3 and Fe_3O_4 flower-like hollow microspheres*, J. Solid State Chem. **199** (2013) 204.

[7] Y. El Mendili, J. F. Bardeau, N. Randrianantoandro, J. M. Greneche and F. Grasset, *Structural behavior of laser-irradiated γ-Fe_2O_3 nanocrystals dispersed in porous silica matrix: γ-Fe_2O_3 to α-Fe_2O_3 phase transition and formation of ε-Fe_2O_3*, STAM **17** (2016) 597.

[8] R. M. Fratila, S. Rivera-Fernandez and J. M. de La Fuente, *Shape matters: synthesis and biomedical applications of high aspect ratio magnetic nanomaterials*, Nanoscale **7** (2015) 8233.

[9] T. Wang, Y. Xu, W. Ling, A. Mosa, S. Liu, Z. Lin, H. Wang and X. Hu, *Dissemination of antibiotic resistance genes is regulated by iron oxides: Insight into the influence on bacterial transformation*, Environ. Int. (2024) 108499.

[10] J. Sun, S. Zhou, P. Hou, Y. Yang, J. Weng, X. Li and M. Li, *Synthesis and characterization of biocompatible Fe_3O_4 nanoparticles*, J. Biomed. Mater. Res. Part A **80** (2007) 333.

[11] Y. Y. Xu, L. Wang, T. Wu and R. M. Wang, *Magnetic properties of α-Fe_2O_3 nanopallets*, Rare Metals **38** (2019) 14.

[12] J. N. Park, P. Zhang, Y. S. Hu and E. W. McFarland, *Synthesis and characterization of sintering-resistant silica-encapsulated Fe_3O_4 magnetic nanoparticles active for oxidation and chemical looping combustion*, Nanotechnol. **21** (2010) 225708.

[13] B. D. L. Mendes and A. Kontny, *Restoration and transformation: The response of shocked and oxidized magnetite to temperature*, J. Geophys. Res. Solid Earth **129**(2) (2024) e2023JB027244.

[14] L. E. Lagoeiro, *Transformation of magnetite to hematite and its influence on the dissolution of iron oxide minerals*, J. Metamorph. Geol. **16** (2024) 415.
[15] J. Ning, P. Gao, S. Yuan, Y. Han, Y. Sun and W. Li, *Highly efficient and green separation of iron from complex low-grade polymetallic ore via hydrogen-based mineral phase transformation*, Powder Technol. **433** (2024) 119177.
[16] U. S. Khan, A. Manan, N. Khan, A. Mahmood and A. Rahim, *Transformation mechanism of magnetite nanoparticles*, Mater. Sci.-Poland **33** (2015) 278.
[17] G. Kletetschka, P. J. Wasilewski and P. T. Taylor, *Hematite vs. magnetite as the signature for planetary magnetic anomalies?*, Phys. Earth Planet. Inter. **119** (2000) 259.
[18] S. S. Pati, L. H. Singh, J. M. Ochoa, E. M. Guimarãesa, M. J. A. Sales, J. A. H. Coaquira, A. C. Oliveira and V. K. Garg, *Facile approach to suppress γ-Fe_2O_3 to α-Fe_2O_3 phase transition beyond 600˚C in Fe_3O_4 nanoparticles*, Mater. Res. Express **2** (2015) 045003.
[19] X. Guoxi and X. Yuebin, *Effects on magnetic properties of different metal ions substitution cobalt ferrites synthesis by sol-gel auto-combustion route using used batteries*, Mater. Lett. **164** (2016) 444.
[20] S. Y. Kazemi, P. Biparva and R. Pourfaraj, *Self-synthesis of superparamagnetic α-Fe_2O_3 and Fe_3O_4 nanoparticles: an eco-friendly and economic process*, J. Iran. Chem. Soc. **18** (2021) 3399.
[21] F. Fiévet, S. Ammar-Merah, R. Brayner, F. Chau, M. Giraud, F. Mammeri, J. Peron, J. Y. Piquemal, L. Sicard and G. Viau, *The polyol process: a unique method for easy access to metal nanoparticles with tailored sizes, shapes and compositions*, Chem. Soc. Rev. **47** (2018) 5187.
[22] N. V. Long, N. T. Nhat Hang and H. V. Cuu, *Micro/nanosized ferrite and hexaferrite structures: The polyol processes for synthesis*, Int. J. Nanomater. Nanotechnol. Nanomed. **9** (2023) 024.
[23] N. V. Long, N. T. N. Hang, Y. Yang and M. Nogami, *Synthesis of cobalt and its metallic magnetic nanoparticles*, Handbook of Magnetic Hybrid Nanoalloys and their Nanocomposites, Cham: Springer International Publishing (2022).
[24] R. C. Pullar, *Hexagonal ferrites: A review of the synthesis, properties and applications of hexaferrite ceramics*, Prog. Mater. Sci. **57** (2022) 1191.
[25] Y. Tian, D. Wu, X. Jia, B. Yu and S. Zhan, *Core-shell nanostructure of α-Fe_2O_3/Fe_3O_4: synthesis and photocatalysis for methyl orange*, J. Nanomater. **2011** (2011) 837123.
[26] H. M. Z. H. El Ghandoor, H. M. Zidan, M. M. Khalil and M. I. M. Ismail, *Synthesis and some physical properties of magnetite (Fe_3O_4) nanoparticles*, Int. J. Electrochem. Sci. **7** (2012) 5734.
[27] L. Li, C. He, W. Lei, P. Gao and T. Lei, *In situ synthesis of Fe_2O_3/Fe_3O_4 nanoarray hybrid as highly effective electrocatalysts for alkaline hydrogen evolution*, J. Alloys Compd. **978** (2024) 173501.
[28] X. H. Liu, W. B. Cui, W. Liu, X. G. Zhao, D. Li and Z. D. Zhang, *Exchange bias and phase transformation in α-Fe_2O_3/Fe_3O_4 nanocomposites*, J. Alloys Compd. **475**(1-2) (2009) 42.
[29] J. Ji, Y. Huang, J. Yin, X. Zhao, X. Cheng, S. He, X. Li, J. He and J. Liu, *Synthesis and electromagnetic and microwave absorption properties of monodispersive Fe_3O_4/α-Fe_2O_3 composites*, ACS Appl. Nano Mater. **1**(8) (2018) 3935.
[30] T. Arun, K. Prabakaran, R. Udayabhaskar, R. V. Mangalaraja and A. Akbari-Fakhrabadi, *Carbon decorated octahedral shaped Fe_3O_4 and α-Fe_2O_3 magnetic hybrid nanomaterials for next generation supercapacitor applications*, Appl. Surf. Sci. **485** (2019) 147.
[31] N. V. Long, Y. Yang, C. M. Thi, N. Van Minh, Y. Cao and M. Nogami, *The development of mixture, alloy, and core-shell nanocatalysts with nanomaterial supports for energy conversion in low-temperature fuel cells*, Nano Energy **2** (2013) 636.
[32] N. V. Long, Y. Yang, M. Yuasa, C. M. Thi, Y. Cao, T. Nann and M. Nogami, *Controlled synthesis and characterization of iron oxide nanostructures with potential applications for gas sensors and the environment*, RSC Adv. **4** (2014) 6383.
[33] N. V. Long, Y. Yang, T. Teranishi, C. M. Thi, Y Cao and M. Nogami, *Synthesis and magnetism of hierarchical iron oxide particles*, Mater. Design **86** (2015) 797.
[34] A. Jafari, S.F. Shayesteh, M. Salouti, and K. Boustani, *Effect of annealing temperature on magnetic phase transition in Fe_3O_4 nanoparticles*, J. Magn. Magn. Mater. **379** (2015) 305.
[35] S. B. Attanayake, A. Chanda, R. Das, M. H. Phan and H. Srikanth, *Effects of annealing temperature on the magnetic properties of highly crystalline biphase iron oxide nanorods*, AIP Adv. **13** (2023) 025333.